Front. Environ. Sci. Eng. 2022, 16(12): 160
https://doi.org/10.1007/s11783-022-1595-7

RESEARCH ARTICLE

Effect of loading rate on shear strength parameters of mechanically and biologically treated waste

Guoyang Fan, Zhenying Zhang (✉), Jiahe Zhang, Jiayue Zhang, Qiaona Wang, Min Wang, Bang Wang, Chengyu Nie

School of Civil Engineering and Architecture, Zhejiang Sci-tech University, Hangzhou 310018, China

HIGHLIGHTS

- Mechanical behavior of MBT waste affected by loading rate was investigated.
- Shear strength ratio of MBT waste increases with an increase in loading rate.
- Cohesion is inversely related to loading rate.
- Internal friction angles are positively related to loading rate.
- MBT waste from China shows smaller range of φ.

GRAPHIC ABSTRACT

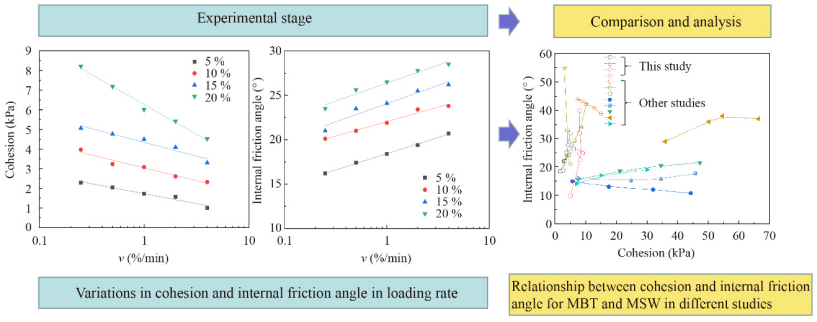

ARTICLE INFO

Article history:
Received 23 January 2022
Revised 31 May 2022
Accepted 31 May 2022
Available online 9 July 2022

Keywords:
Mechanically and biologically treated waste
Landfill
Triaxial test
Loading rate
Axial strain
Shear strength parameter

ABSTRACT

Mechanical biological treatment (MBT) technology has attracted increasing attention because it can reduce the volume of waste produced. To deal with the current trend of increasing waste, MBT practices are being adopted to address waste generated in developing urban societies. In this study, a total of 20 specimens of consolidated undrained triaxial tests were conducted on waste obtained from the Hangzhou Tianziling landfill, China, to evaluate the effect of loading rate on the shear strength parameters of MBT waste. The MBT waste samples exhibited an evident strain-hardening behavior, and no peak was observed even when the axial strain exceeded 25%. Further, the shear strength increased with an increase in the loading rate; the effect of loading rate on shear strength under a low confining pressure was greater than that under a high confining pressure. Furthermore, the shear strength parameters of MBT waste were related to the loading rate. The relationship between the cohesion, internal friction angle, and logarithm of the loading rate could be fitted to a linear relationship, which was established in this study. Finally, the ranges of shear strength parameters cohesion c and effective cohesion c' were determined as 1.0–8.2 kPa and 2.1–14.9 kPa, respectively; the ranges of the internal friction angle φ and effective internal friction angle φ' were determined as 16.2°–29° and 19.8°–43.9°, respectively. These results could be used as a valuable reference for conducting stability analyses of MBT landfills.

1 Introduction

Landfilling is a common and effective method for disposing of municipal solid waste (MSW) (Ke et al., 2017; Ramaiah and Ramana, 2017; Falamaki et al., 2022). However, the phenomenon of waste siege caused by growing populations (especially in developing countries) and the rapid exhaustion of available processing spaces have led to severe environmental problems (Zhang et al., 2020; Lu et al., 2022). Available data show that approximately 2.01 billion tons of MSW were generated globally in 2016, which is expected to increase to 3.4 billion tons by 2050 (Kaza et al., 2018). In this context, pretreating large amounts of waste is beneficial for reducing the biodegradability of MSW, as the number of potential pollutants lost in leachate and fugitive greenhouse gas emissions can be reduced (Bhandari and Powrie, 2013). Many countries prohibit landfilling unpretreated MSW (e.g., EU landfill directive (EC, 1999)).

✉ Corresponding author
E-mail: zhangzhenyinga@163.com

Mechanical biological treatment (MBT) is a pretreatment method that is increasingly being adopted by developing countries to reduce the volume of waste produced. The MBT process converts MSW containing high amounts of organic matter into MBT waste using mechanical technology (e.g., mechanical crushing and screening), biological treatment technology (e.g., aerobic or anaerobic digestion), or both. However, some reinforcing elements within the waste (e.g., wooden sticks, metals, textiles, and other materials) are reduced by MBT technology, and such changes can affect the stability of the landfill where the final product (MBT waste) is disposed (Petrovic, 2016). Therefore, it is necessary to select an appropriate shear strength parameter and conduct stability analyses when constructing landfill sites. Thus, the shear strength of the MBT waste needs to be determined.

Many previous studies have evaluated the shear strength characteristics of MSW through laboratory and field tests. Stoll (1971) was the first to evaluate the mechanical characteristics of MSW and provide many associated insights. Over the following decades it was found that MSW materials exhibit significant strain-hardening properties (Gabr and Valero, 1995; Grisolia et al., 1995; Reddy et al., 2009; Zekkos et al., 2010; Pulat and Yukselen-Aksoy, 2017; Falamaki et al., 2020). Degraded and aged waste was found to have greater shear strength (Van Impe, 1998; Harris et al., 2006; Cho et al., 2011), and some studies determined that shear strength increased with an increased loading rate (Zekkos et al, 2007; Bray et al., 2009; Karimpour-Fard et al., 2011).

Fibrous materials play a role in enhancing the shear strength of MBT waste and reinforcing the soil (De Lamare Neto, 2004; Fucale, 2005; Calle, 2007; Pimolthai and Wagner, 2014; Fucale et al., 2015). The shear strength characteristics of MSW are input into a database, and information is collected. The shear strength parameters of MSW and MBT waste are listed in Table S1.

Several studies have investigated the shear strength characteristics of MBT waste, which are mainly related to the fiber content, confining pressure, unit weight, and particle size. Some researchers used a direct shear test to study the shear strength characteristics of MBT waste (Kölsch, 1995; Powrie and Beaven, 1999; Fernando, 2011) and obtained the corresponding shear strength parameters under a certain strain condition. Through the analysis of experimental data, Kölsch (1995) reported that shear strength comprises the frictional force on the shear surface and tensile force in the fiber; Fernando (2011) concluded that moisture content has no significant effect on the strength of MBT waste, and materials with higher unit weight have greater shear strength. Many other researchers used triaxial tests to study the shear strength characteristics of MBT waste (Bhandari and Powrie, 2013; Babu et al., 2015; Lakshmikanthan et al., 2018). Babu et al. (2015) found that the shear strength of the waste increased with an increase in the unit weight. Samples with a higher unit weight exhibited a higher shear strength than samples with lower values. Lakshmikanthan et al. (2018) stated that the shear strength parameters increased with an increase in axial strain.

Shear strength is related to the loading rate for both the traditional soil (Lefebvre and LeBoeuf, 1987; Díaz-Rodríguez et al., 2009) and the MSW (Zekkos et al., 2007; Bray et al., 2009; Karimpour-Fard et al., 2011). Therefore, a systematic study of the relationship between the shear strength of MBT waste and loading rate is both interesting and promising. MBT waste is gradually landfilled in layers at varying rates based on the waste output. We determined that shear strength will increase the processing and landfill rates when the quantity of MBT waste is large. The rates decrease with a decrease in MBT quantity. A faster landfilling rate leads to a faster file up of waste with a steeper slope. A landfilled waste pile is affected by the lateral earth pressure caused by another such pile that is located nearby, which causes lateral sliding. Simultaneously, the rapid piling of the waste can cause slipping and instability at the bottom of the landfilled waste. The main reason for instability slip is that the shear stress on the potential slip surface exceeds the shear strength of MBT waste; the landfilling rate has a critical influence on the shear strength parameters (cohesion and internal friction angle) of the MBT waste. If the shear strength parameters of the MBT waste are not selected appropriately, it is easy to cause errors in the design of the landfill pile, which can lead to instability and slip in the MBT waste landfill. Researchers have been tasked with providing suitable shear strength parameters for the MBT landfill and guide the landfilling rate of the MBT waste to ensure the stability of the MBT landfill and prevent the collapse and destruction of the landfill. We conducted triaxial tests in a laboratory setting at five loading rates (0.25 %/min, 0.5 %/min, 1 %/min, 2 %/min, and 4 %/min) and established the correlation between the shear strength parameters (cohesion and internal friction angle) and the loading rate to simulate the effect of the MBT waste landfilling rate on its shear strength parameters. The test results could be used as a valuable reference for conducting stability analyses of MBT landfills.

2 Materials and methods

2.1 Test materials

The MBT waste analyzed in this study (shown in Fig. S1(a)) was obtained from the Tianziling landfill site, which is a standard valley landfill located in Hangzhou on the southeast coast of China. The average moisture content of the waste was 18.5 % and the specific gravity was 1.53. The components of the MBT waste as dry mass are listed in Table S2. According to the technical specification for

soil test of landfilled municipal solid waste in China (Xue et al., 2013), the maximum particle size of the test material was limited to one-eighth of the sample diameter for minimizing the influence of size. The MBT waste was sieved through a 7.725-mm mesh to obtain test materials, as illustrated in Fig. S1(b).

2.2 Sample preparation

Dried materials were rescreened to abrade sharp particles such as wood, stone, and metal to prevent them from tearing or puncturing the latex membranes. Samples were prepared in a cylindrical mold measuring 61.8 mm in diameter and 125 mm in height. For easy molding, water was added to the materials for them to attain a moisture content of 50 %. The sample was divided into five layers within the mold. Each layer was compacted from a constant height with a 3-kg rammer to avoid delamination of the sample, before filling the next layer of waste. The surface of each layer was scratched gently with a spatula; the process was repeated until the sample was finished. To prevent the samples from rebounding or loosening after demolding, they were sealed for one week before demolding.

2.3 Testing apparatus

The triaxial test apparatus (STSZ-ZD) is composed of a pressure chamber, a confining pressure control system, a backpressure control system, a pore pressure measurement system, a testing machine, and a pressure measurement device, which is manufactured and improved by Zhejiang Geotechnical Instrument Limited, China. The control ranges of the confining and back pressures are both 0–1 MPa (with an accuracy of 0.001 kPa); the pressure is pumped into the pressure chamber by pumping hydraulics. Pre-pressuring was conducted before each test to eliminate residual bubbles in the pipeline and minimize the experimental error. The testing machine controls the axial force in a range of 0–30 kN (with an accuracy of 0.0001 kN). A drain hole was positioned next to the pressure chamber to measure the drainage volume of the sample; the bottom of the chamber was connected to the axial pressure control system to enable the application of axial pressure.

2.4 Test design and procedure

The consolidated undrained test method was adopted and conducted under pressures of 50, 100, 200, and 300 kPa. The loading rates were set to 0.25 %/min, 0.5 %/min, 1 %/min, 2 %/min, and 4 %/min of the initial sample height. Table 1 presents the test plan. The sample wrapped in a latex membrane was placed in the pressure chamber, head saturation was applied, and a confining pressure of 20 kPa was introduced. Simultaneously, the height of the inlet pipe was increased to ensure a 1 m liquid level difference between the inlet and base outlet pipes. Water was passed through the sample from the bottom to the top until the water output and water input per unit time were equal. Backpressure saturation was applied after the completion of the head saturation; a confining pressure of 20 kPa was then applied to the sample, and the pore pressure valve was opened. When the pore pressure stabilized, the reading was recorded, and the pore pressure valve was closed. Backpressure and confining pressure were applied in stages, and the pressure increment for each stage was 30 kPa. Further, the pore pressure was recorded at each stable pressure stage. When the rate of the increase caused by the confining pressure and back pressure was greater than 0.98 at a certain level of pressure, the saturation was considered complete.

The drain valve was opened and a controlled application of 50 kPa confining pressure was applied to consolidate the sample. The drain valve was closed after the pore pressure dissipated, and the volume of the discharged liquid was measured. A constant confining pressure was maintained, and the axial force was applied at a loading rate of 0.25 %/min until the end of the test. The sample was then removed and replaced with another sample; the tests were conducted at loading rates of 0.5 %/min, 1 %/min, 2 %/min, and 4 %/min under the same confining pressure. The above steps were repeated, and the tests were conducted under confining pressures of 100, 200, and 300 kPa with loading rates of 0.25 %/min, 0.5 %/min, 1 %/min, 2 %/min,

Table 1 Test plan for consolidated undrained test

Sample number	Confining pressure (kPa)	Initial void ratio	Loading rate (%/min) [a)]	Initial unit weight (kN/m^3)
A-1	50	2.0	0.25	7.6
A-2	50	2.0	0.5	7.6
A-3	50	2.0	1	7.6
A-4	50	2.0	2	7.6
A-5	50	2.0	4	7.6
B-1	100	2.0	0.25	7.6
B-2	100	2.0	0.5	7.6
B-3	100	2.0	1	7.6
B-4	100	2.0	2	7.6
B-5	100	2.0	4	7.6
C-1	200	2.0	0.25	7.6
C-2	200	2.0	0.5	7.6
C-3	200	2.0	1	7.6
C-4	200	2.0	2	7.6
C-5	200	2.0	4	7.6
D-1	300	2.0	0.25	7.6
D-2	300	2.0	0.5	7.6
D-3	300	2.0	1	7.6
D-4	300	2.0	2	7.6
D-5	300	2.0	4	7.6

Notes: a) 0.25 % (0.3125 mm/min), 0.5 % (0.625 mm/min), 1 % (1.25 mm/min), 2 % (2.5 mm/min), 4 % (5 mm/min).

and 4 %/min, respectively. The readings of the displacement gauge, pore pressure gauge, and dynamometer were obtained to determine the deformation of the sample.

3 Results

Changes in the sample in relation to the test are illustrated in Fig. S2. Fig. S2(a) shows the sample before the test; Fig. S2(b) shows the sample during the test, where the latex membrane is close to the sample under the confining pressure; and Fig. S2(c) shows the sample condition after the test is completed. Oblique crack surface failure did not occur although compression and bulging are evident.

3.1 Effect of changes in confining pressure

Considering a loading rate of 1 %/min as an example, relationships between the deviator stress and axial strain at confining pressures of 50, 100, 200, and 300 kPa are shown in Fig. 1.

The deviator stress increased with an increase in the strain, which shows the strain-hardening characteristics; no peak was observed at the 25 % strain level. The figure shows that the growth trend of the deviator stress was different for different confining pressures. Under the confining pressures of 200 and 300 kPa, the deviator stress was roughly divided into two stages: the first stage occurred before 10 % axial strain, and it was the rapid growth stage of deviator stress and the initial stage of axial deformation. Axial pressure was applied to the consolidated sample, and the internal pores of the sample were reduced; the particles were closely interconnected to directly provide resistance to deformation. In the second stage, the deviator stress continued to increase after an axial strain of 10 %. The reason for this phenomenon may be related to the compressibility of waste particles as the direct resistance of particles to deformation reached its maximum in the first stage. Owing to shearing dislocation, particles began to move into the surrounding loose and porous materials and between the residual pores. Filamentary and strip-like fiber-like reinforced materials inside the sample were well anchored with the surrounding particles; the friction between the particles and elasticity of the fiber-reinforced material worked together to resist axial deformation, as described by Shariatmadari et al. (2009). This is well represented as the "growth trend" of the deviator stress in the stress-strain curve. Under confining pressures of 50 and 100 kPa, the deviator stress increased rapidly up to within 3 % of axial strain; however, it showed a slowly increasing trend after the axial strain exceeded 3 %.

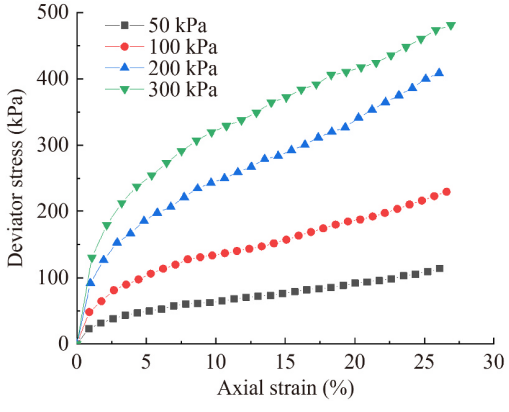

Fig. 1 Relationship between deviator stress and axial strain at 1 %/min loading rate.

When the axial strain was constant, the deviator stress increased with an increase in the confining pressure. This may have been caused by the following: with an increase in the confining pressure, the interior of the sample became tighter, the void ratio reduced, and the occlusion between particles became closer; this led to an increase in material stiffness and a resistance to deformation. This indicates that the shear strength of waste at the bottom of the MBT landfill was considerably greater than that of the upper layer. This phenomenon indicates that compaction applied before landfilling effectively increased the stability of the landfill and played a critical role in expanding landfill capacity.

3.2 Effect of changes in the loading rate

Tests were conducted under confining pressures of 50, 100, 200, and 300 kPa with loading rates of 0.25 %/min, 0.5 %/min, 1 %/min, 2 %/min, and 4 %/min. Relationships between the deviator stress and axial strain of MBT waste are presented in Fig. 2, where it is evident that the deviator stress increases in different ranges with an increase in the loading rate.

The fitting line between the shear strength and logarithmic loading rate is shown in Fig. 3, where Figs. 3(a) and 3(b) show the relationship between shear strength and logarithmic loading rate at an axial strain of 10% and 20%, respectively.

As shown in Fig. 3, at axial strains of 10 % and 20 %, the shear strength of MBT waste increased with an increase in the logarithmic loading rate; a linear relationship is evident. This behavior can be attributed to the shear behavior immediately entering the second stage when the loading rate increased which reduced the dislocation behavior of the components and reduced deformation inside the material. The fiber-embedded mixture immediately acted as a direct resistance to deformation resulting in greater stiffness and shear strength. This premise is consistent with the previous MSW test results of Karimpour-Fard et al. (2011). In addition, Anderson and Kavazanjian (1995) pointed out that less creep and relative displacement of the waste constituents will occur in the refuse under short-term loading conditions, which will result in higher stiffness and shear strength.

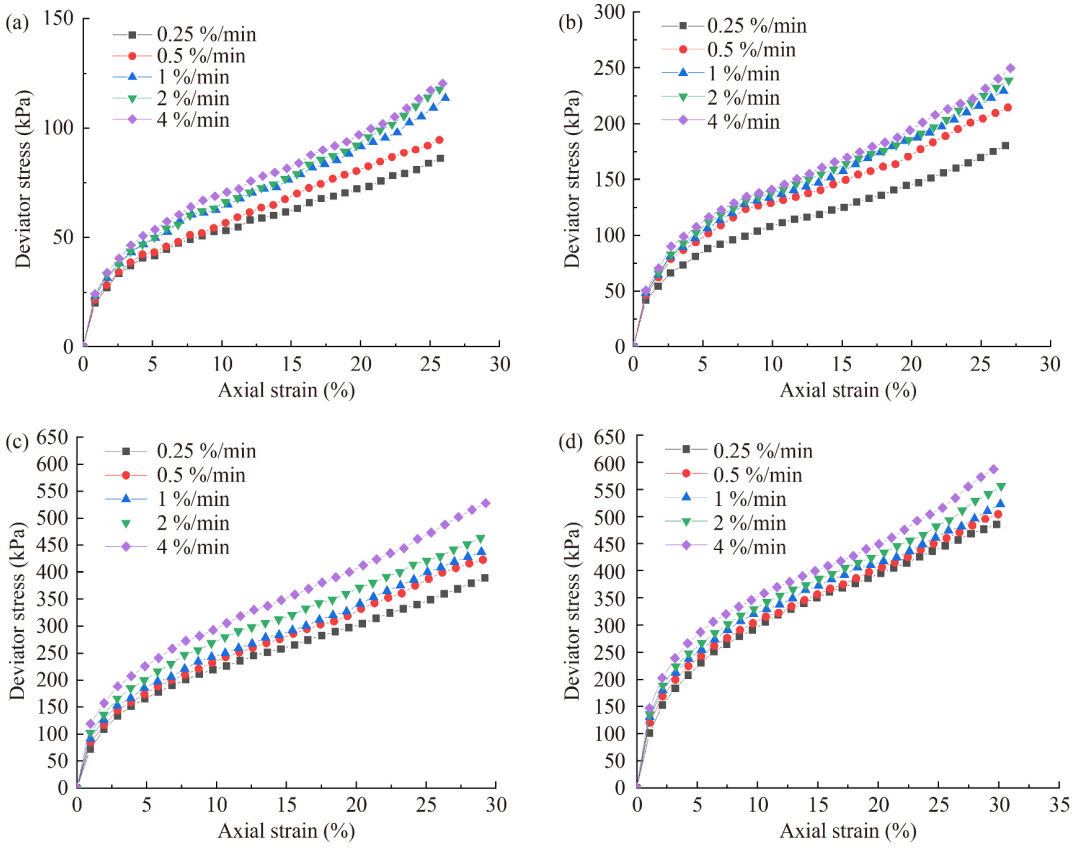

Fig. 2 Relationship between deviator stress and axial strain under different confining pressures: (a) 50; (b) 100; (c) 200; and (d) 300 kPa.

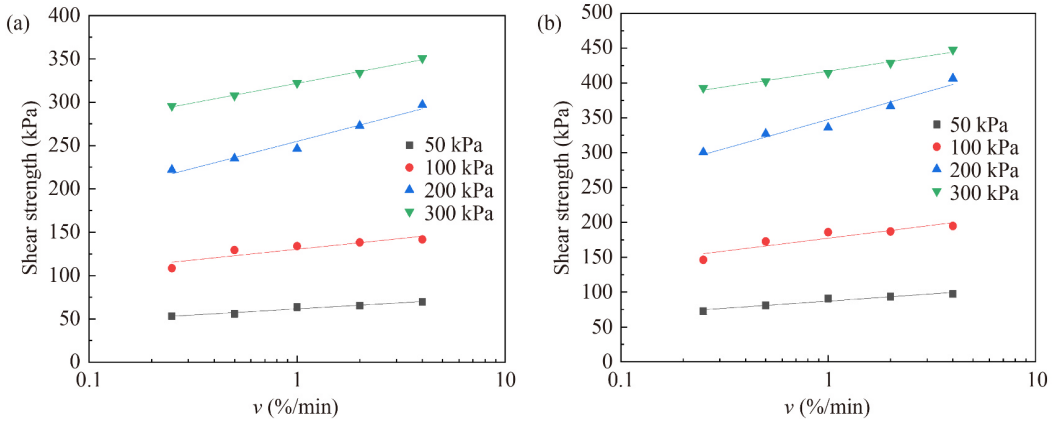

Fig. 3 Relationship between shear strength and logarithmic loading rate at a axial strain of (a) 10 % and (b) 20 %.

The fitted linear functions for different axial strains are given by

$$\tau_{f10\%} = A + B\lg v, \quad (1)$$

where $\tau_{f10\%}$ represents the shear strength at 10% axial strain, v represents the loading rate, and A and B denote the coefficients,

$$\tau_{f20\%} = C + D\lg v, \quad (2)$$

where $\tau_{f20\%}$ represents the shear strength at 20 % axial strain, and C and D represent the coefficients. Coefficients A and B and C and D, and the correlation coefficient R^2 are also listed in Tables S3 and S4, respectively.

The shear strength ratio is defined as the ratio that corresponds to the other loading rates and the shear strength corresponding to the benchmark loading rate (0.25 %/min). Relationships between the shear strength ratio and logarithmic loading rate at 10 % and 20 % axial strain are shown in Figs. 4(a) and 4(b), respectively.

Fig. 4 shows that although the relationship between shear strength ratio and logarithmic loading rate of MBT

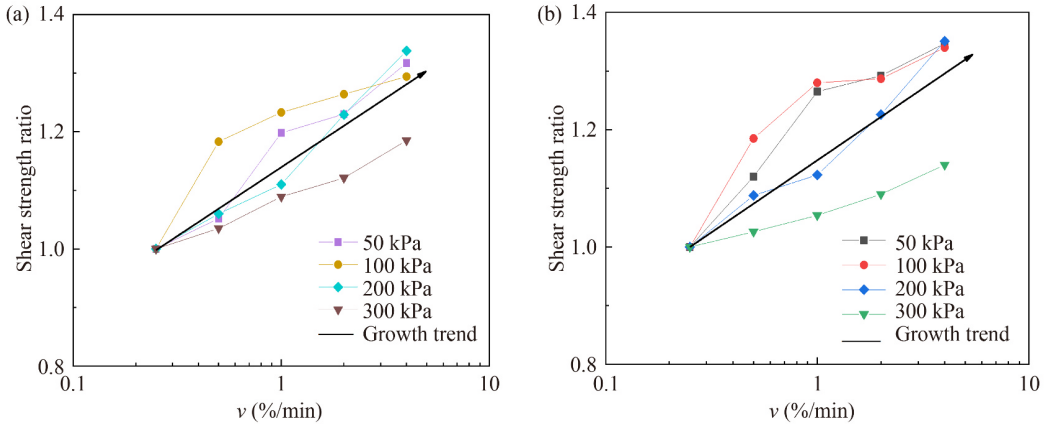

Fig. 4 Relationship between shear strength ratio and loading rate at an axial strain of (a) 10 % and (b) 20 %.

waste is not a simple monotonic function, there is an evident tendency for the ratio to increase with an increase in the logarithmic loading rate. At confining pressures of 50, 100, and 200 kPa, the shear strength increased by approximately 30 % when the rate was increased from the benchmark loading rate of 0.25 %/min to 4 %/min, whereas at 300 kPa it increased only by approximately 15 %; this could be due to the higher confining pressure. The particles in the material were occluded to a sufficient density, and the enhancement effect relating to the increased loading rate reduced the internal displacement phenomenon of the material; therefore, the denser material had a relatively small effect on the loading rate. Compared with a 10 % axial strain, the shear strength enhancement effect caused by an increased loading rate was more conspicuous at 20 % axial strain as more aggregates resisted deformation during the larger shearing behavior. Zekkos et al. (2007) used a variable loading rate shear test with dynamic shear at an increased loading rate of 100 times (from 0.5 %/min to 50 %/min). Based on a series of considerations, the dynamic shear strength of MSW was found to be approximately 30% higher than the static shear strength. This study compares the effect of a constant loading rate on shear strength under different strains; it was found that when the rate increased 16 times, the shear strength increased to 14%–35% (compared with 0.25 %/min). The shear strength of MBT waste increases with an increase in the loading rate, but the actual landfill project tends to be unsafe under the larger landfill rate, this can easily lead to instability and destruction of the landfill (increased loads on the foundation, steepening of the landfill, increased leachate production, large safety factor, among others). Therefore, it is very important to study the influence of the loading rate.

3.3 Variations in shear strength parameters

3.3.1 Variations in cohesion with changes in loading rate

As there is no conspicuous peak in the MBT waste stress-strain curve, shear strength parameters are based on shear stress at 5 % or 10 % axial strain; 15 % or 20 % axial strains are occasionally used. Strength envelopes with 5 %, 10 %, 15 %, and 20 % axial strains are shown in Fig. S3 (1 %/min loading rate is used as an example in Fig. S3). Figs. S3(a)–S3(d) show strength envelopes with 5 %, 10 %, 15 %, and 20 % axial strain, respectively, and the other loading rate strength envelopes are drawn similarly.

According to the strength envelope, the values of cohesion c and effective cohesion c' can be obtained; these are shown in Table S5.

Furthermore, cohesion (c), effective cohesion (c'), and logarithmic loading rate fitting line are shown in Fig. 5. Figs. 5(a) and 5(b) show the relationship between cohesion and the logarithmic loading rate and effective cohesion and the logarithmic loading rate, respectively.

Fig. 5 shows that when the strain is unchanged, both c and c' decrease with an increase in the loading rate. When the loading rate increases from 0.25 %/min to 4 %/min, the decrease rate of c is 44.2 % and the reduction rate of c' is 45 %. The reason for this may be as follows: according to the relationship between particles (Kralchevsky and Nagayama, 1994; Butt and Kappl, 2009), the internal particles of waste materials are a special type of colloidal particles. The mutual attraction between particles in the material plays a key role in cohesion; this includes electrostatic attraction, van der Waals force, and cementation between particles. In soil mechanics, their values directly affect cohesion (Li, 2016). However, this relationship between particles also exists in MBT waste. An increase in the loading rate destroys this mutual attraction between particles to a certain extent and causes a decrease in both c and c'.

The fitted linear functions are given as

$$c = E + F \lg v, \tag{3}$$

$$c' = G + H \lg v, \tag{4}$$

where c represents cohesion, c' is effective cohesion, and E, F, G, and H denote the coefficients. Coefficients E and

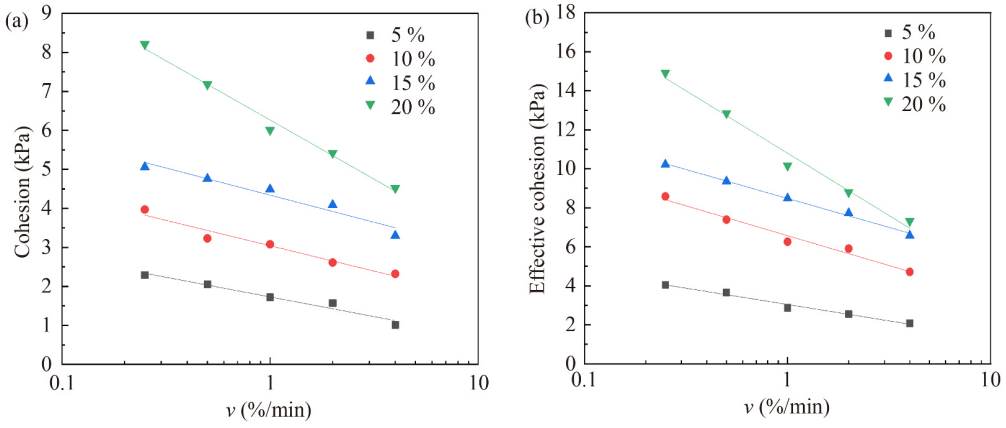

Fig. 5 Relationship between shear strength parameters and loading rate (cohesion and effective cohesion): (a) relationship between cohesion and loading rate; (b) relationship between effective cohesion and loading rate.

F and the correlation coefficient R^2 are shown in Table S6, and coefficients G and H and the correlation coefficient R^2 are shown in Table S7.

3.3.2 Variations in internal friction angle with changes in loading rate

The strength envelope is drawn with 5 %, 10 %, 15 %, and 20 % axial strain. According to the strength envelope, the values of the internal friction angle φ and effective internal friction angle φ' are obtained and listed in Table S8.

The internal friction angle (φ), effective internal friction angle (φ'), and logarithmic loading rate fitting line are shown in Fig. 6. Fig. 6(a) shows the relationship between the internal friction angle and logarithmic loading rate; Fig. 6(b) shows the relationship between the effective internal friction angle and logarithmic loading rate.

The fitted linear functions are obtained via

$$\varphi = I + J \lg v, \tag{5}$$

$$\varphi' = K + L \lg v, \tag{6}$$

where φ denotes the internal friction angle, φ' denotes the effective internal friction angle, and I, J, K, and L are the coefficients.

Coefficients I and J and the correlation coefficient R^2 are listed in Table S9, and coefficients K and L and correlation coefficient R^2 are listed in Table S10.

Fig. 6 shows that at constant strain, both φ and φ' increase with an increase in the loading rate. When the loading rate increases from 0.25%/min to 4% per/min, the growth rate of φ is 25.1%; the growth rate of φ' is 12.9%. This phenomenon may be attributed to the dilatancy behavior in the center of the sample during the shearing process. Shear force provides the required energy for the dilatancy behavior in the form of work, and in the microscopic view, it is manifested as an increase in the angle of internal friction. Li (2016) stated in soil mechanics that the contact surface of particles is rough and uneven, and the friction formed when sliding against each other is sliding friction; when the particles that bite each other move relatively, the part of the force that binds

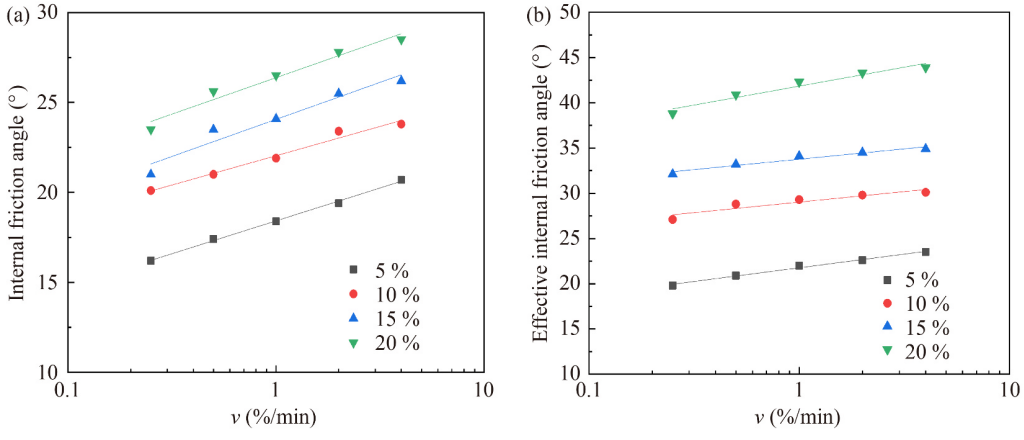

Fig. 6 Relationship between shear strength parameters and logarithmic loading rate (internal friction angle and effective internal friction angle): (a) relationship between internal friction angle and logarithmic loading rate; (b) relationship between effective internal friction angle and logarithmic loading rate.

them is the occlusal friction. When the material is sheared and deformed, the particles that bite together move relatively, and one of the particles must be lifted from the original position or sheared to move across the adjacent particles; therefore, the original state between the particles must be destroyed. The denser the material, the smaller the roundness of the particles, the stronger the occlusion between the particles, and the larger values of φ and φ'. Similarly, MBT waste particles exhibit sliding friction and occlusal friction during the loading process. When the loading rate increases, the shearing behavior becomes faster and the material becomes denser faster. The greater the friction between the particles, the greater the values of φ and φ'.

3.3.3 Variations in shear strength parameters with changes in axial strain

Relationships between the cohesion, internal friction angle, and axial strain of MBT waste at different loading rates are shown in Fig. 7.

Fig. 7(a) shows the relationship between cohesion and axial strain; Fig. 7(b), effective cohesion and axial strain; Fig. 7(c), internal friction angle and axial strain; and Fig. 7(d), effective internal friction angle and axial strain. These results indicate that the cohesion and internal friction angle of MBT waste are positively correlated with the axial strain. As the shearing process progresses, a more conspicuous increase appears in the growth trend between φ and φ' compared to c and c'. Further, the growth rate of c', φ' is evidently greater than the growth rate of c and φ; this occurred because the pore water pressure approached the confining pressure along the shear process. The results in Tables S5 and S8 show that the value ranges of the shear strength parameters c, c', φ, and φ' of the consolidated undrained triaxial MBT waste are 1.0–8.2 kPa, 2.1–14.9 kPa, 16.2°–29°, and 19.8°–43.9°, respectively.

4 Discussion

The corresponding relationships between the cohesion and internal friction angle relating to the shear strength parameters of MSW and MBT waste obtained in this study and other studies are shown in Fig. 8.

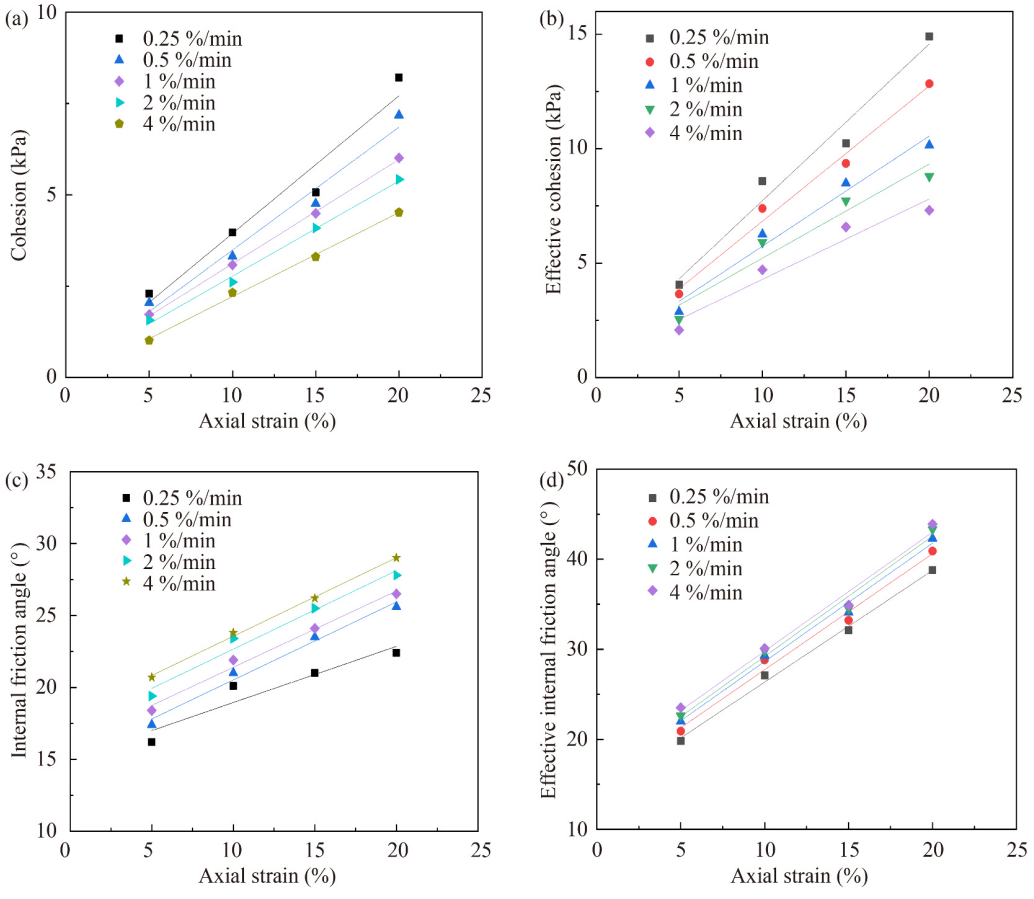

Fig. 7 Relationship between shear strength parameters and axial strain: (a) relationship between cohesion and axial strain; (b) relationship between effective cohesion and axial strain; (c) relationship between internal friction angle and axial strain; (d) relationship between effective internal friction angle and axial strain.

Fig. 8 shows that the variation range in the MBT waste cohesion is narrow with 0–10 kPa and 0–15 kPa distribution ranges at the total and effective stresses, respectively. However, the internal friction angle varies widely having 10°–40° and 20°–55° distribution ranges at the total and effective stresses, respectively. In addition, the cohesion of MSW has a large variation range (between 5–70 kPa), and the internal friction angle again varies between 10°–40°. The figure also shows that the distribution ranges of cohesion obtained by Machado et al. (2002), Feng (2005), and Reddy et al. (2009) for MSW are relatively close (between 5–50 kPa).

The fitting line for the shear strength parameters of MBT waste mostly lies on the left of that of MSW, which implies the cohesion of MSW is greater than that of MBT waste. This can be because of the differences between countries conducting the tests and the MSW and MBT waste disposal methods, and it results in different waste components. The moisture and organic matter contents of MSW are higher; as the organic content decreases, its shear strength parameters tend to move closer to that of MBT waste. The shear strength parameters obtained in this paper (consolidated undrained test, total stress, 20% strain,) are between the results of Babu et al. (2015) and Lakshmikanthan et al. (2018). There are minimal differences in the range of cohesion for the three studies; however, the range of the internal friction angle is relatively large. In the study of the axial strain effect, the fitting line of shear strength parameters from the consolidated undrained test in this paper is similar to that of Lakshmikanthan et al. (2018). A comparison of the effective stress parameters from the consolidated drained test of Babu et al. (2015) and those from the consolidated undrained test in this study indicates that the effective internal friction angle range of Babu et al. (2015) is wider and the effective cohesion range is smaller.

Fig. 8 shows that it is difficult to clearly define a relationship between cohesion and the internal friction angle that changes with the conditions. In this study, the cohesion decreased with an increase in the loading rate and internal friction angle under constant axial strain. Under a constant loading rate, the internal friction angle increased with an increase in axial strain and cohesion. Reddy et al. (2009) observed that with an increase in axial strain, the internal friction angle decreased with an increase in cohesion. The results of Babu et al. (2015) showed that under different particle sizes and unit weights, cohesion increased with an increase in the internal friction angle in the consolidated undrained test and decreased with an increase in the internal friction angle in the consolidated drained test. The results of Machado et al. (2002), Feng (2005), Zhao et al. (2014), and Lakshmikanthan et al. (2018) showed that the internal friction angle increased with an increase in axial strain and cohesion.

The differences between the study results can be attributed to the following:

1) There are differences between the ages of the waste materials employed in the different studies. Reddy et al. (2009) used fresh MSW, Feng (2005) used five years old MSW, and Machado et al. (2002) and Zhao et al. (2014) used materials that were more than 10 years old. This

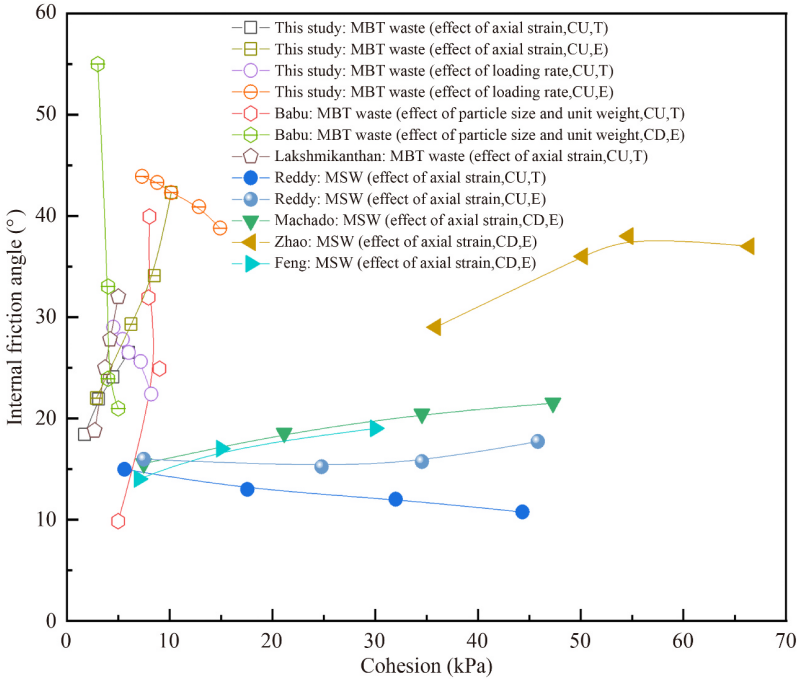

Fig. 8 Relationship between cohesion and internal friction angle for MBT and MSW in different studies. (CU- consolidated undrained Test, CD- consolidated drainage Tests, T- total stress parameters, and E- effective stress parameters).

study and that of Babu et al. (2015) and Lakshmikanthan et al. (2018) used MBT waste. It is established that age strongly affects the shear strength characteristics of the materials, and the effect of degradation and upper load on the material is more pronounced as the material ages. Pulat and Yukselen-Aksoy (2017) reported that compared with fresh waste samples, aged waste has a lower organic content, greater inorganic content, lower cohesion value, and relatively larger internal friction angle. Harris et al. (2006) provided similar conclusions. Furthermore, Cañizal et al. (2011) reported that degradation and aging affect the shear strength of waste by reducing cohesion and increasing the internal friction angle.

2) There are differences between the triaxial test methods employed in the different studies. The shear strength parameter results of Reddy et al. (2009), Babu et al. (2015), Lakshmikanthan et al. (2018), and this study, which were obtained from consolidated undrained (CU) tests are shown in Fig. 8. However, studies by Machado et al. (2002), Feng (2005), Zhao et al. (2014), and Babu et al. (2015) relate to shear strength parameters obtained from consolidated drained (CD) tests. The shear strength characteristics of waste can be studied under both short-term and long-term conditions. The short-term conditions represent the landfill construction phase and are often referred to as undrained conditions in the geotechnical engineering literature. Such cases are related to the destruction of landfills during or after rainfall. In contrast, the drainage strength refers to the stability of the landfill under long-term conditions (Lakshmikanthan et al, 2018). Both the CU and CD tests are loaded after the specimen is consolidated; however, compared with the CU test, the CD test is loaded vertically under drainage conditions that require a relatively slow loading rate. The loading rate is a factor that affects the strength parameters, and therefore, the effective stress parameters of Babu et al. (2015) CD test are different from the effective stress parameters of the CU test in this study. In addition, Vilar and Carvalho (2005) stated that the effective stress shear strength parameters of the CU test are inconsistent with those of the CD test.

3) Differences between particle sizes and the sizes of samples used in the studies. The particle size of samples used in this study was < 7.725 mm; Babu et al. (2015) used particle sizes of 4 mm and 10 mm; Reddy et al. (2009) used particle sizes of 0.75–40 mm, and Lakshmikanthan et al. (2018) used particle sizes of < 20 mm. The effect of particle size on shear strength has been extensively studied (Jessberger et al., 1995; Casagrande et al., 2006; Consoli et al., 2007). The results of Jessberger et al. (1995) indicate that particle size may influence the shear strength of the waste. Based on the test results of Babu et al. (2015), the shear strength of two different particle sizes showed conspicuous differences. Further, the sample sizes used in this study and the studies of Machado et al. (2002), Zhao et al. (2014), and Babu et al. (2015) were 61.8 mm × 125 mm, 100 mm × 200 mm, 200 mm × 400 mm, and 500 mm × 300 mm, respectively. Owing to the high heterogeneity of waste, the differences in sample sizes cause differences in the composition of the internal materials, and this affects the shear strength parameters of the waste.

5 Conclusions

In this study, a series of consolidated undrained tests were conducted and the shear strength parameters of 20 specimens of MBT waste were studied. The following conclusions can be drawn from the results of this study:

1) MBT waste is a highly compressible material with a complex composition. The deviator stress showed no peak, even when axial strain exceeded 25%; this provides evidence for strain-hardening characteristics.

2) The shear strength of MBT waste increased with an increase in the loading rate. There was an evident linear relationship between shear strength and the logarithm of the loading rate; an expression for the linear relationship between the shear strength and the logarithm of the loading rate was established. The reason for this behavior can be attributed to the shear properties immediately entering the second stage when the loading rate was increased, which reduced the dislocation of the components and deformation inside the material. The fiber-embedded mixture immediately provided direct resistance to the deformation, and this resulted in greater stiffness and shear strength.

3) The shear strength ratio of MBT waste increased with an increase in the loading rate. An increase from the benchmark loading rate of 0.25% per min to 4% per min (equivalent to 16 times the loading rate) caused an approximate increase of 30% in the shear strength of the MBT waste. The enhancement effect of increasing the loading rate can be explained by the reduction in the dislocation of the components as the increase in the shear strength of the waste corresponds to an increase in the shear strength ratio.

4) The cohesion and effective cohesion of MBT waste decreased with an increase in the loading rate. The relationships between cohesion, effective cohesion, and the logarithm of the loading rate were fitted to linear relationships. The mutual attraction between particles in the material played a key role in cohesion as an increase in the loading rate reduces the mutual attraction (electrostatic attraction, van der Waals force, and cementation) to a certain extent, which causes a decrease in c and c'.

5) Internal friction angle and effective internal friction angle of MBT waste increased with an increase in the loading rate. Linear relationships were established between the internal friction angle, effective internal friction angle, and the logarithm of the loading rate. As

the shearing action progresses, the particles slide relative to each other, and the waste particles that bite together also move relative to each other. The movement requires one particle to be sheared or staggered from the original position, and therefore, the original state between particles needs to be changed. The increase in the loading rate accelerates the shear behavior as the specimen is compacted faster, and the internal particles are tighter. Increased occlusion between the particles causes an increase in φ and φ'.

6) The shear strength parameters of MBT waste were found to be related to axial strain. Cohesion, effective cohesion, internal friction angle, and effective internal friction angle all increased with an increase in axial strain and ranges 1.0–8.2 kPa, 2.1–14.9 kPa, 16.2°–29°, and 19.8°–43.9°, respectively.

These conclusions are only drawn from our laboratory tests. The MBT waste materials used were obtained from Hangzhou, China, and may, therefore, not be representative of other places. However, our predictive framework allows for the identification of the underlying mechanisms that control the stability of MBT landfills and provides insights for improving the efficacy of waste management. Moreover, we prove that shear strength parameters can be used as a valuable reference for conducting stability analyses of MBT landfills.

Acknowledgements This research was funded by the National Natural Science Foundation of China (Nos. 51978625 and 51678532) and the Zhejiang Provincial Natural Science Foundation of China (No. LZ21E080003). The authors are grateful for the assistance provided by the Hangzhou Environmental Group, China.

Electronic Supplementary Material Supplementary material is available in the online version of this article at https://doi.org/10.1007/s11783-022-1595-7 and is accessible for authorized users.

References

Anderson D G, Kavazanjian E Jr (1995). Performance of landfills under seismic loading. In: Proceedings of the 3rd International Conference on Recent Advances in Geotechnical Earthquake Engineering and Soil Dynamics, Missouri. Colombia: University of Missouri-Rolla, 277–306

Babu G L S, Lakshmikanthan P, Santhosh L G (2015). Shear strength characteristics of mechanically biologically treated municipal solid waste (MBT-MSW) from Bangalore. Waste Management, 39: 63–70

Bhandari A R, Powrie W (2013). Behavior of an MBT waste in monotonic triaxial shear tests. Waste Management, 33(4): 881–891

Bray J, Zekkos D, Kavazanjian E Jr, Athanasopoulos G, Riemer M (2009). Shear strength of municipal solid waste. Journal of Geotechnical and Geoenvironmental Engineering, 135(6): 709–722

Butt H J, Kappl M (2009). Normal capillary forces. Advances in Colloid and Interface Science, 146(1−2): 48–60

Calle J A C (2007). Geomechanical behavior of urban solid waste. Dissertation for the Doctoral Degree. Rio de Janeiro: Federal University of Rio de Janeiro

Cañizal J, Lapeña P, Castro J, Costa A, Sagaseta C (2011). Determination of shear strength of MSW. Field tests vs. laboratory tests. In: 4th International Workshop "Hydro-Physico-Mechanics of Landfills," Santander. Santander: University of Cantabria, 3005–3008

Casagrande M D T, Coop M R, Consoli N C (2006). Behavior of a fiber reinforced bentonite at large shear displacements. Journal of Geotechnical and Geoenvironmental Engineering, 132(11): 1505–1508

Cho Y M, Ko J H, Chi L, Townsend T G (2011). Food waste impact on municipal solid waste angle of internal friction. Waste Management, 31(1): 26–32

Consoli N C, Casagrande M D T, Coop M R (2007). Performance of a fibre-reinforced sand at large shear strains. Geotechnique, 57(9): 751–756

De Lamare Neto A (2004). Shearing resistance of urban solid waste and granular materials with fibers. Dissertation for the Doctoral Degree. Rio de Janeiro: Federal University of Rio de Janeiro

Díaz-Rodríguez J A, Martínez-Vasquez J J, Santamarina J C (2009). Strain-rate effects in Mexico City soil. Journal of Geotechnical and Geoenvironmental Engineering, 135(2): 300–305

EC (1999). Council Directive 1999/31/EC of 26 April 1999 on the Landfill of Waste. Official Journal of the European Communities, 182: 1–19

Falamaki A, Ghareh S, Homaee M, Hamtaeipour S A, Abedpour S, Kiani S, Mousavi N, Rezaei M, Taghizadeh M M, Dehbozorgi M, Nouri A (2020). Laboratory shear strength measurements of municipal solid waste at room and simulated in situ landfill temperature, Barmshoor Landfill, Iran. International Journal of Civil Engineering, 18(2): 185–197

Falamaki A, Homaee M, Baneshi Z, Salari M (2022). Simulating effect of potassium carbonate on quantity and quality of municipal solid waste leachate. International Journal of Civil Engineering, 20(2): 185–194

Feng S J (2005). Static and dynamic strength properties of municipal solid waste and stability analyses of landfill. Dissertation for the Doctoral Degree. Hangzhou: Zhejiang University (in Chinese)

Fernando V I (2011). Shear strength characteristics of mechanically biologically treated (MBT) waste. Dissertation for the Doctoral Degree. Hampshire: University of Southampton

Fucale S, Jucá J F T, Muennich K (2015). The mechanical behavior of MBT–waste. Electron Journal of Geotechnical and Geoenvironmental Engineering, 20(13): 5927–5937

Fucale S P (2005). Influence of the reinforcement components in the resistance of municipal solid waste. Dissertation for the Doctoral Degree. Recife: Federal Univesrity of Pernambuco

Gabr M A, Valero S N (1995). Geotechnical properties of municipal solid waste. Geotechnical Testing Journal, 18(2): 241–251

Grisolia M, Napoleoni Q, Tangredi G (1995). The use of triaxial tests for the mechanical characterization of municipal solid waste. In: Proceedings of the 5th International Landfill Symposium-Sardinia. Cagliari, Italy: CISA, Environmental Sanitary Engineering Centre, 761–767

Harris J M, Shafer A L, DeGroff W, Hater G R, Gabr M A, Bariaz M

(2006). Shear strength of degraded reconstituted municipal solid waste. Geotechnical Testing Journal, 29(2): 141–148

Jessberger H L, Syllwasschy O, Kockel R (1995). Investigation of waste body behaviour and waste structure interaction. In: Proceedings of the 5th International Landfill Symposium-Sardinia. Cagliari, Italy: CISA, Environmental Sanitary Engineering Centre, 731–743

Karimpour-Fard M, Machado S L, Shariatmadari N, Noorzad A (2011). A laboratory study on the MSW mechanical behavior in triaxial apparatus. Waste Management, 31(8): 1807–1819

Kaza S, Yao L, Bhada-Tata P, Woerden F V (2018). What a waste 2.0: A global snapshot of solid waste management to 2050. Washington, DC: World Bank Publications

Ke H, Hu J, Xu X B, Wang W F, Chen Y M, Zhan L T (2017). Evolution of saturated hydraulic conductivity with compression and degradation for municipal solid waste. Waste Management, 65: 63–74

Kölsch F (1995). Material values for some mechanical properties of domestic waste. In: Proceedings of the 5th International Landfill Symposium-Sardinia. Cagliari, Italy: CISA, Environmental Sanitary Engineering Centre, 711–729

Kralchevsky P A, Nagayama K (1994). Capillary forces between colloidal particles. Langmuir, 10(1): 23–36

Lakshmikanthan P, Sughosh P, Babu G L S (2018). Studies on characterization of mechanically biologically treated waste from Bangalore city. Indian Geotechnical Journal, 48(2): 293–304

Lefebvre G, LeBoeuf D (1987). Rate effects and cyclic loading of sensitive clays. Journal of Geotechnical Engineering, 113(5): 476–489

Li G X (2016). Strength of soils. In: Li G X, ed. Advanced Soil Mechanics. 2nd ed. Beijing: Tsinghua University Press, 140–146 (in Chinese)

Lu W, Huo W, Gulina H, Pan C (2022). Development of machine learning multi-city model for municipal solid waste generation prediction. Frontiers of Environmental Science & Engineering, 16(9): 119

Machado S L, Carvalho M F, Vilar O M (2002). Constitutive model for municipal solid waste. Journal of Geotechnical and Geoenvironmental Engineering, 128(11): 940–951

Petrovic I (2016). Mini-review of the geotechnical parameters of municipal solid waste: Mechanical and biological pre-treated versus raw untreated waste. Waste Management & Research, 34(9): 840–850

Pimolthai P, Wagner J F (2014). Soil mechanical properties of MBT waste from Luxembourg, Germany and Thailand. Songklanakarin Journal of Science and Technology, 36(6): 701–709

Powrie W, Beaven R P (1999). Hydraulic properties of household waste and implications for landfills. Geotechnical Engineering, 137(4): 235–247

Pulat H F, Yukselen-Aksoy Y (2017). Factors affecting the shear strength behavior of municipal solid wastes. Waste Management, 69: 215–224

Ramaiah B J, Ramana G V (2017). Study of stress-strain and volume change behavior of emplaced municipal solid waste using large-scale triaxial testing. Waste Management, 63: 366–379

Reddy K R, Hettiarachchi H, Parakalla N S, Gangathulasi J, Bogner J E (2009). Geotechnical properties of fresh municipal solid waste at Orchard Hills Landfill, USA. Waste Management, 29(2): 952–959

Shariatmadari N, Machado S L, Noorzad A, Karimpour-Fard M (2009). Municipal solid waste effective stress analysis. Waste Management, 29(12): 2918–2930

Stoll O W (1971). Mechanical properties of milled refuse. Phoenix, Arizona: ASCE National Water Resources Engineering Meeting, 11–15

Van Impe W F (1998). Environmental geotechnics: ITC 5 activities, state of art. In: Proceedings of the 3rd International Congress on Environmental Geotechnics. Lisbon, Portugal: Balkema, 1163–1187

Vilar O M, Carvalho M F (2005). Shear strength and consolidation properties of municipal solid waste. In: International Workshop on Hydro-Physico-Mechanics of Landfills. Grenoble, France: Grenoble 1 University, 21–22

Xue Q, Li J S, Zhao Y, Chen Z L, Feng X T, Ma S P, Deng Z G, Liu Y, Lu H J, Liu X L, Chen X Y, Xie W G (2013). Technical Specification for Soil Test of Landfilled Municipal Solid Waste CJJ/T204-2013. Beijing: China Architecture and Building Press (in Chinese)

Zekkos D, Athanasopoulos G A, Bray J D, Grizi A, Theodoratos A (2010). Large-scale direct shear testing of municipal solid waste. Waste Management, 30(8-9): 1544–1555

Zekkos D, Bray J D, Athanasopoulos G A, Riemer M F, Kavazanjian E, Founta X, Grizi A (2007). Compositional and loading rate effects on the shear strength of municipal solid waste. In: Proceedings of the 4th International conference on earthquake geotechnical engineering. Thessaloniki, Greece: Springer, 25–28

Zhang Z Y, Wang Y X, Fang Y H, Pan X F, Zhang J H, Xu H (2020). Global study on slope instability modes based on 62 municipal solid waste landfills. Waste Management & Research, 38(12): 1389–1404

Zhao Y R, Xie Q, Wang G L, Zhang Y J, Zhang Y X, Su W (2014). A study of shear strength properties of municipal solid waste in Chongqing landfill, China. Environmental Science and Pollution Research International, 21(22): 12605–12615